Long-lived transient behavior in an n^+-n-n^+ semiconductor device with optical stochasticity

Yuo-Hsien Shiau
Department of Physics, National Dong Hwa University, 1, Sec 2, Da-Hsueh Road, Shou-Feng, Hualien 974, Taiwan, Republic of China

Yih-Ferng Peng
Department of Civil Engineering, National Chi-Nan University, Taiwan, Republic of China
(Received 6 April 2004; revised manuscript received 31 January 2005; published 28 June 2005)

We numerically study the response time of an ultrafast microwave switch, i.e., a GaAs-based Gunn device, under stochastic stimuli. The conducting states in this semiconductor device can be controlled in the presence of laser illumination near the doping notch. With the consideration of the additional randomness in laser intensity, the switching time from the initial unstable state to the final stable state will increase. Therefore, the so-called noise delayed decay of unstable states in an n^+-n-n^+ semiconductor device is demonstrated.

DOI: 10.1103/PhysRevE.71.066216 PACS number(s): 05.45.−a, 05.70.Ln, 72.20.Ht, 89.75.Kd

I. INTRODUCTION

The studies of transport properties in semiconductors have made great progress in recent decades. This is mainly due to the advanced technologies for development of new materials [1,2] and the application of nonlinear dynamics to the fundamental well-known materials [3–5]. The new materials, e.g., quantum-confinement semiconductors, indeed shed light on the semiconductor industry, which may invoke industry revolution at the beginning of the 21st century. On the other hand, the discipline of nonlinear dynamics [6] also grows fast, which is due to the cooperation of theoretical background and experimental findings. The unique property in nonlinear dynamics is about universality, e.g., chaos observed among different disciplines, which is not system-dependent. Among the systems considered, semiconductors represent interesting and highly productive examples of the experimental investigation of nonlinear dynamics. This is due to the fact that nonlinear transport theory of carriers in semiconductors is fundamentally well known, so that reliable theoretical models can be constructed and the underlying physics may be fully understood. Therefore, semiconductors are ideal systems to compare nonlinear theory and experimental findings. In practice, nonlinear behaviors in semiconductors are very useful to design electronic devices such as microwave generators, switches, memory devices, etc.

Recently, extensive theoretical and experimental studies conducted for the purpose of development and optimization of various Gunn diodes have been reported. These studies focus mostly on the enhancement of output power and/or increasing microwave frequency for short Gunn devices [7,8]. In this article, we report the electrical response with a long-lived transient characteristic, i.e., the lock-on effect, in a GaAs-based Gunn device under stochastic stimuli. Our results can be considered as numerical evidence for the new development of nonlinear theory, which describes the so-called noise-delayed decay (NDD) of unstable dynamical states [9,10]. Furthermore, this nonequilibrium decay process in our system can be used to control the response time of an ultrafast microwave switch (i.e., a nanosecond switch). To the best of our knowledge, the nonequilibrium decay rate in realistic semiconductors influenced by optical stochasticity has never been reported. Moreover, the concept of NDD can be generally applied to other semiconductor systems with unstable dynamical states. For example, semiconductors with persistent photoconductivity can be used in many important applications. However the locking time of the dark current (i.e., an unstable dynamical state) is fundamentally related to material preparation [11]. According to the NDD effect, the locking time can possibly be prolonged and controlled. Therefore, the NDD effect developed by the nonlinear theory may play a crucial role for the semiconductor industry.

II. THE MODEL

Our simulated model is based on the well-known drift diffusion equations for electrons and holes [12]. Due to the consideration of optical excitation, the generation-recombination processes shall include optical generation of electron-hole pairs with rate g and recombination of electron-hole pairs with rate γ. G_{ii} means the generation of electron-hole pairs via impact ionization. Therefore, the dynamical equations we simulate are the Poisson equation, the continuity equations of electrons and holes, and the equation for total current density J,

$$\frac{\partial^2 \phi}{\partial x^2} = \frac{e}{\epsilon}[p + N_D(x) - n], \tag{1}$$

$$\frac{\partial n}{\partial t} + \frac{\partial J_n}{\partial x} = gI(x) + G_{ii} - \gamma np, \tag{2}$$

$$\frac{\partial p}{\partial t} + \frac{\partial J_p}{\partial x} = gI(x) + G_{ii} - \gamma np, \tag{3}$$

$$J(t) = -eJ_n + eJ_p + \epsilon \frac{\partial E}{\partial t}, \tag{4}$$

where G_{ii} and the particle current densities for electrons J_n and holes J_p are defined as

$$J_n = nv_n(E) - D_n \frac{\partial n}{\partial x}, \tag{5}$$

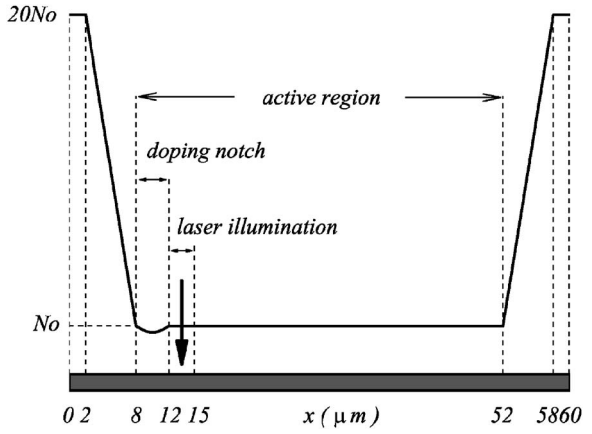

FIG. 1. Schematic illustration of device doping profile $N_D(x)$ and local laser illumination $I(x)$. The active region is sandwiched between the highly doped n^+ cathode and anode region. A doping notch is located at the beginning of the active region. Cathode and anode are connected with an external dc bias which is fixed at 12 V.

$$J_p = -p\mu_p E - D_p \frac{\partial p}{\partial x}, \tag{6}$$

$$G_{ii} = g_0 \exp\left[-\left(\frac{E_{\text{th}}}{E}\right)^2\right](|J_n| + |J_p|), \tag{7}$$

and e is the elementary charge. $\epsilon, \mu_p, D_n, D_p, g_0$, and E_{th} denote dielectric constant, hole mobility, diffusion coefficient of electron, diffusion coefficient of hole, rate of impact ionization, and threshold field for impact ionization, respectively. There are two spatial-dependent parameters $N_D(x)$ and $I(x)$, respectively, which correspond to the doping profile of an n^+-n-n^+ GaAs sandwich structure [13] and local uniform laser illumination in the active region (Fig. 1). The motivation of the consideration of local optical excitation is to redistribute the space-charge field around the doping notch via optical generation of hole carriers. More precisely, local optical excitation will make the doping notch a collector of electrons. Then, the internal field in the doping notch will become stronger, which can speed up the electrons and influences the dipole-domain nucleation. The three independent dynamical variables in these coupled equations are free-electron density n, free-hole density p, and electric potential ϕ, where the electric field E is equal to $-\partial\phi/\partial x$. It is worthwhile to mention that the electron drift velocity $v_n(E)$ is determined by a single electron temperature mode [14] which describes the energy relaxation process for electrons and establishes the relation between local electric field and carrier heating. The formulations are

$$E^2 = \frac{3k}{2e\tau_e}(T_e - T_L)\frac{1 + R\exp\left(-\frac{\Delta E}{kT_e}\right)}{\mu_1 + \mu_2 R\exp\left(-\frac{\Delta E}{kT_e}\right)}, \tag{8}$$

$$v_n(E) = \frac{\mu_1 + \mu_2 R\exp\left(-\frac{\Delta E}{kT_e}\right)}{1 + R\exp\left(-\frac{\Delta E}{kT_e}\right)}E, \tag{9}$$

where μ_1 and μ_2 are the electron mobility at the lower and the upper valleys, respectively, ΔE is the energy difference between the two valleys, T_L is the lattice temperature, τ_e is the energy relaxation time, k is the Boltzmann constant, and R is the ratio of the density of states for the upper valley to the lower valley. The parameters used in our simulation are listed in Table I. Besides, the boundary conditions used to simulate Eqs. (1)–(9) are that the hole density at the cathode and anode are set to be zero, the electron density at the cathode and anode are equal to the doping density of the n^+ region (i.e., $20N_0$), and the grounded cathode is considered. In the following, the detailed numerical results are computed and demonstrated by using Eqs. (1)–(9) together with boundary conditions.

III. NUMERICAL RESULTS AND DISCUSSIONS

Before we demonstrate the NDD effect in our model system, it shall be pointed out why a GaAs-based Gunn device can be treated as an inverter of optical input to microwave output [15] and can be considered as an ultrafast microwave switch. Figure 2 illustrates the different current oscillations when this semiconductor device is illuminated at higher and lower laser intensity. The underlying physics for these two different current oscillations is due to the formation of different electric-field domains. One is the optically induced transit domain [Fig. 3(a)] and the other is the optically induced quenched domain [Fig. 3(b)] [16]. If we turn off the

TABLE I. The fundamental constants and GaAs parameters for numerical simulation.

Parameter	Value	Parameter	Value
D_n	200 cm^2/s	R	94
D_p	20 cm^2/s	k	8.6186×10^{-5} eV/K
ϵ	1.17×10^{-12} F/cm	ΔE	0.31 eV
e	1.61×10^{-19} C	T_L	300 K
g	4.4×10^{18} cm^{-1} s^{-1} W^{-1}	τ_e	10^{-12} s
γ	10^{-10} s^{-1} cm^3	N_0	5×10^{15} cm^{-3}
μ_1	8500 $\text{cm}^2/\text{V s}$	g_0	2×10^5 cm^{-1}
μ_2	50 $\text{cm}^2/\text{V s}$	E_{th}	550 kV/cm
μ_p	400 $\text{cm}^2/\text{V s}$		

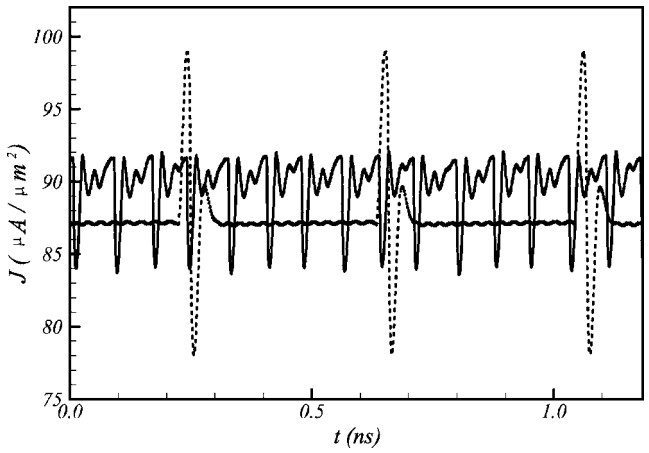

FIG. 2. Time evolution plot of the total current density for laser intensity at 125 kW/cm^2 (dashed line) and 115 kW/cm^2 (solid line).

laser stimulation, the traditional quenched domain is observed in Fig. 3(c). It shall be noted that the optically induced instability (or bifurcation) can be observed in Fig. 3(b), which is compared with the spatiotemporal dynamics in Fig. 3(c). Such an instability will eventually lead to the domain transition when the laser intensity is large enough, i.e., a transition would occur from Fig. 3(b) to Fig. 3(a). Furthermore, these two optically induced domains can coexist under the same laser intensity. And the transition between these two dynamical states is hysteretic. Therefore, the optically induced hysteretic switching between different conducting states exists in this n^+-n-n^+ semiconductor device. Besides, the transition regions are numerically observed at which laser intensities equal 122 kW/cm^2 and 77 kW/cm^2. And these two laser intensities correspond to the transition from optically induced quenched domain to transit domain and vice versa, respectively. The upper portion of Fig. 4 illustrates the transient current oscillation from the optically induced quenched domain to transit domain with the laser intensity initially at 115 kW/cm^2 and then increasing suddenly to 125 kW/cm^2. The time location of the first extreme maximum current density for the optically induced transit domain is defined as the switching time $T_{q\to t}$ from the optically induced quenched to transit domain. The switching time in this case is around 1.9 ns. This is why a GaAs-based Gunn device can be regarded as an ultrafast microwave switch. If we further consider the additional weak noise in the laser intensity, the local uniform laser illumination $I(x)$ shall be replaced by $I(x)[1+A\,\eta(t)]$ with an additional requirement $1+A\,\eta(t)\geqslant 0$. Here A is the strength of the noise and $\eta(t)$ must satisfy the white noise conditions: $\langle \eta(t)\rangle=0$ and $\langle \eta(t)\,\eta(t')\rangle=\delta(t-t')$. The symbol $\langle\rangle$ denotes the ensemble average. The lower portion of Fig. 4 demonstrates that the switching time is increased to 3.5 ns with $A=10^{-2}$. It shall be noted that the additional randomness is just given at laser intensity being equal to 125 kW/cm^2 for the artificial control of electrical response. The corresponding spatiotemporal dynamics of Fig. 4 are shown in Fig. 5 via contour plots. The white area represents the higher electric-field values, and intermediate shading from gray to black shows different levels of lower

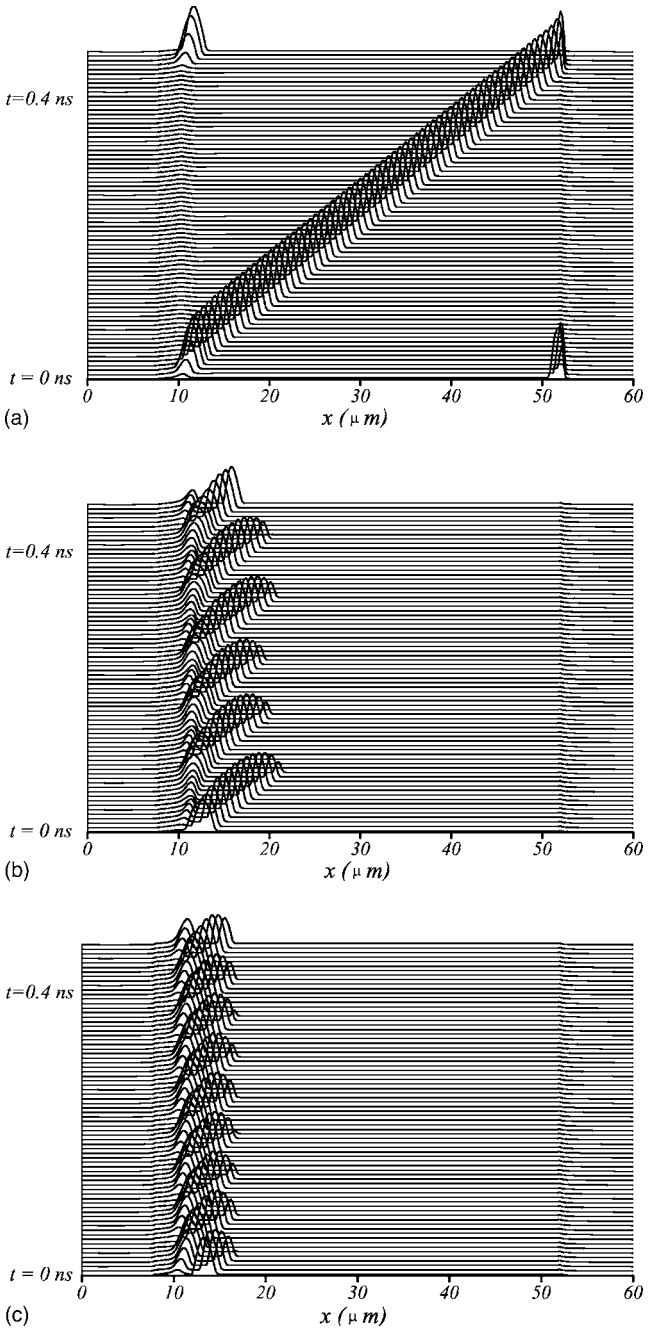

FIG. 3. The spatiotemporal behaviors of electric-field domains for laser intensity at (a) 125 kW/cm^2, (b) 115 kW/cm^2, and (c) 0 kW/cm^2.

electric-field values. It is seen clearly that the optically induced quenched domain temporally locks in the space, which is strongly dependent on the additional randomness. The detailed relation between $T_{q\to t}$ and A is plotted with squared symbols in Fig. 6. It is interesting to find the prolonged switching time and the nonlinear $T_{q\to t}(A)$ spectrum in Fig. 6. When A exceeds 10^{-2}, the switching time is fixed at 3.5 ns, while the NDD effect disappears as $A\leqslant 10^{-3}$. Now we discuss the switching time $T_{t\to q}$ from the optically induced transit to quenched domain with laser intensity initially at 87 kW/cm^2 and then decreasing suddenly to 76 kW/cm^2.

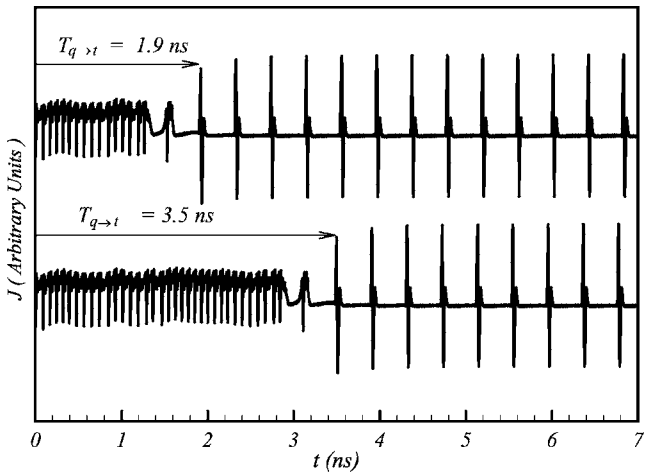

FIG. 4. Time evolution plot of the transient J values for laser intensity beginning at 115 kW/cm^2 and then suddenly increasing to 125 kW/cm^2. The upper portion: without the additional randomness, the switching time $T_{q\to t}$ is 1.9 ns. The lower portion: when A is 10^{-2}, $T_{q\to t}$ is increased to 3.5 ns.

Similarly, the additional randomness is given at which the laser intensity equals 76 kW/cm^2. The $T_{t\to q}(A)$ spectrum, as shown by circle symbols in Fig. 6, displays no NDD effect in this transition branch. The switching time is fixed at 1.3 ns when A is increased from 0 to 10^{-1}.

The findings shown in Fig. 6 can be simply realized via classical attractor dynamics. If the initial conditions were fixed, the phase trajectory from the initial state to the final state and the associated relaxation time, i.e., switching time, can be determined. It is also noted that the dynamical characteristic of the model system, i.e., the phase trajectory and the relaxation time, are not influenced by a small strength of randomness (e.g., A is smaller than 10^{-3}). However, $T_{q\to t}(A)$ and $T_{t\to q}(A)$ exhibit different behaviors with $10^{-3}\leqslant A \leqslant 10^{-1}$. Such a result indicates that the stability of the relaxation path in this system is quite complex. The phase trajectory from the transit mode to the quenched mode still maintains its stability and is not perturbed by the strength of white noise. Nevertheless, it is a different story for the quenched mode to the transit mode. The unstable quenched mode tends to be temporally locked in phase space due to the additional randomness, i.e., noise-enhanced stability for unstable dynamical states. Naively, stronger noise can drive the dynamical system promptly into the convergent regime of the final stable state. Therefore, noise-enhanced stability should be gradually decreased as A is increased. Surprisingly, in the interval of $10^{-2}\leqslant A\leqslant 10^{-1}$, our calculations indicate that there is no sign of increase of $T_{q\to t}$ with respect to A. We believe that the NDD effect shown in the $T_{q\to t}(A)$ spectrum is still an unsolved problem in stochastic processes.

However, these different $T_{q\to t}(A)$ and $T_{t\to q}(A)$ spectra possibly can be explained via local as well as global bifurcation scenarios around the transition points. According to the bifurcation analysis in Ref. [15], catastrophic scenarios can be numerically observed both in the quenched state to the transit state and vice versa. A common situation for catastrophe to arise is where the system undergoes a crisis at

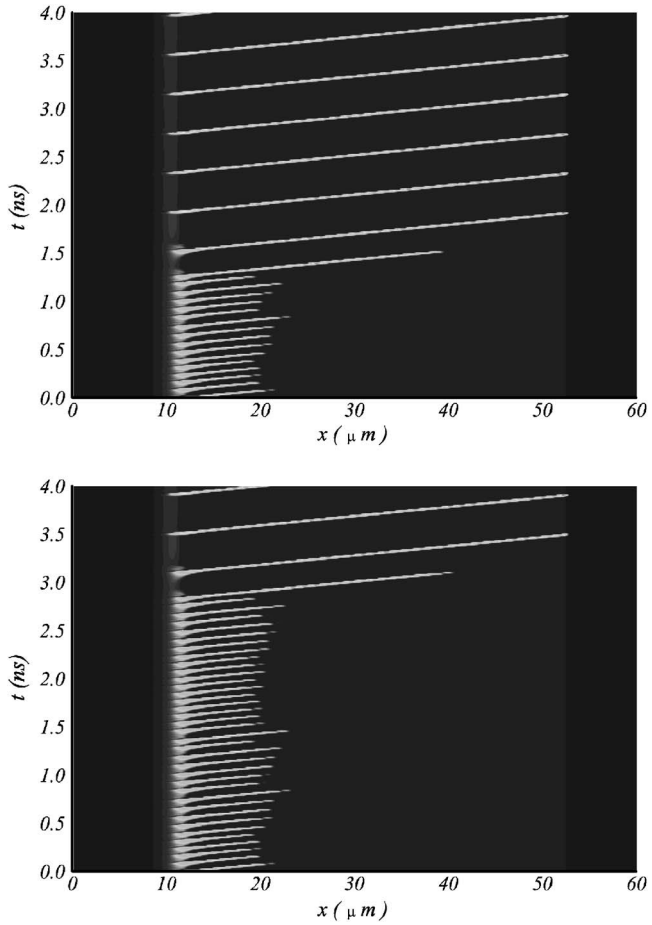

FIG. 5. The contour plots of the spatiotemporal behaviors in Fig. 4 for A being equal to 0 (the upper portion) and 10^{-2} (the lower portion).

which an attractor collides with the basin boundary separating it and another coexisting attractor [17]. If the attractor is chaotic, after the crisis, the chaotic attractor is destroyed and converted into a nonattracting chaotic saddle. A dynamical

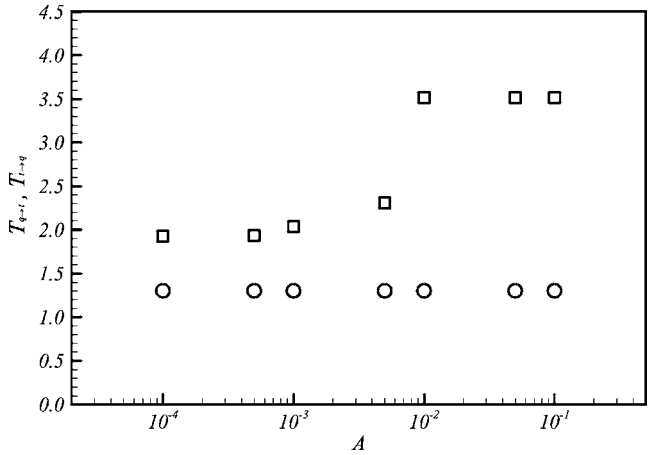

FIG. 6. Illustration of nonlinear $T_{q\to t}(A)$ and flat $T_{t\to q}(A)$ spectra. Please note that the values of $T_{q\to t}(A)$ and $T_{t\to q}(A)$ are obtained from the ensemble average. Each switching time is averaged over 20 different realizations.

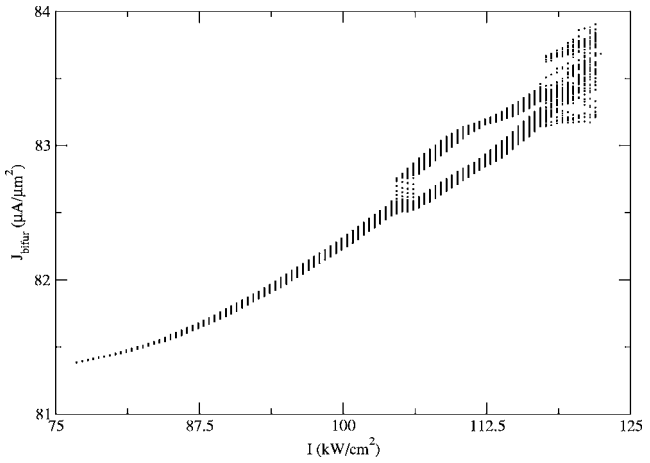

FIG. 7. The bifurcation diagram of J_{bifur} vs I represents the transition from periodic to chaotic quenched domains when laser intensity is increased.

trajectory then wanders in the vicinity of the chaotic saddle for a period of time before it approaches the other attractor. This phenomenon is known as chaotic transient [18,19], which can be realized via the transition from the chaotic quenched state to the periodic transit state in the upper portion of Fig. 5. In order to illustrate the formation of chaotic quenched domains near the transition region with laser intensity being equal to 122 kW/cm^2, the bifurcation diagram of current density with local minimum values J_{bifur} [20] versus laser intensity is illustrated in Fig. 7, which exhibits an incomplete period-doubling scenario. If the laser illumination with randomness is considered, the wandering time in the vicinity of the chaotic saddle will be prolonged and can be realized in the lower portion of Fig. 5. Therefore, the NDD effect in the nonlinear $T_{q\to t}(A)$ spectrum is strongly related with the dynamical structure near the chaotic saddle. If the attractor is periodic, after the crisis, the periodic attractor becomes unstable and quickly approaches another coexisting attractor. The wandering time in this case should be shorter than that of the case in the vicinity of the chaotic saddle. Moreover, the dynamical structure in this case should not be perturbed by the additional weak noise. Therefore, the underlying physics for the $T_{t\to q}(A)$ spectrum with fixed and shorter values also can be interpreted as catastrophe from the periodic transit state to the periodic quenched state.

Finally, we would like to discuss the validity of our approach in the present study. Our simulated model is a combination of the well-known drift diffusion equations, a single electron temperature model, and fixed boundary conditions. To our knowledge, it can successfully describe the domain dynamics for longer devices [14]. The parameters used in this simulation for GaAs are taken from Refs. [12,21], while the coefficients of impact ionization are all from Ref. [22]. Another important issue we would like to discuss is the laser properties. The interesting phenomena in this study occur at laser intensity with the order of magnitude from 10^4 W/cm^2 to 10^5 W/cm^2. As far as we know, such conditions are experimentally feasible since two-wave mixing experiments in GaAs have been performed with light at more than 10 MW/cm^2 intensity [23,24]. And the laser source we considered is a 10-ns-duration pulse of a Nd:YAG laser with wavelength 1064 nm, which ensures that our simulation results, i.e., the switching time from 1.3 ns to 3.5 ns, can be observed in this pulse laser. The technique of 3 μm laser illumination also can be easily performed via GRIN [25], i.e., graded refractive index lenses. Therefore, we believe that our numerical results could be observed experimentally.

IV. CONCLUSIONS

In conclusion, our calculations indicate that an unusual decay process was observed in a nonlinear semiconductor with a bistable characteristic. The decay rate is related to the nonequilibrium process. Furthermore, this nonequilibrium phenomenon can be used to control the response time of an ultrafast microwave switch [26]. We report the electrical response with a long-lived transient characteristic in a GaAs-based Gunn device under stochastic stimuli. Only the switching time $T_{q\to t}$ is strongly enhanced by the optical stochasticity. These results can be considered as numerical evidence for the new development of nonlinear theory which describes the NDD effect for dynamical systems with unstable dynamical states. Besides, we believe that the unification of modern nonlinear theory and practical semiconductor systems can possibly give rise to unique academic interests and novel applications.

ACKNOWLEDGMENTS

This work was supported in part by the National Science Council of the Republic of China (Taiwan) under Contract Nos. NSC 91-2112-M-259-014 and NSC 93-2211-E-260-004.

[1] A. Shik, *Quantum Wells: Physics and Electronics of Two-Dimensional Systems* (World Scientific, Singapore, 1998).

[2] *Theory of Transport Properties of Semiconductor Nanostructures*, edited by E. Schöll (Chapman & Hall, London, 1998).

[3] E. Schöll, *Nonequilibrium Phase Transitions in Semiconductors* (Springer, Berlin, 1987).

[4] F.-J. Niedernostheide, *Nonlinear Dynamics and Pattern Formation in Semiconductors and Devices* (Springer, Berlin, 1995).

[5] *Negative Differential Resistance and Instabilities in 2-D Semiconductors*, edited by N. Balkan, B. K. Ridley, and A. J. Vickers (Plenum, New York, 1993).

[6] H. G. Schuster, *Deterministic Chaos* (Physik-Verlag, Weinheim, 1984).

[7] Y. P. Teoh, G. M. Dunn, N. Priestley, and M. Carr, Semicond. Sci. Technol. **17**, 1090 (2002).

[8] E. Alekseev and D. Pavlidis, Solid-State Electron. **44**, 941 (2000).
[9] V. Horsthemke and R. Lefever, *Noise Induced Transitions* (Springer, Berlin, 1984).
[10] N. V. Agudov and A. N. Malakhov, Phys. Rev. E **60**, 6333 (1999).
[11] R. P. Joshi, P. Kayasit, N. Islam, E. Schamiloglu, C. B. Fleddermann, and J. Schoenberg, J. Appl. Phys. **86**, 3833 (1999).
[12] S. M. Sze, *Physics of Semiconductor Devices* (John Wiley & Sons, New York, 1969).
[13] K. I. Oshio and H. Yahata, J. Phys. Soc. Jpn. **64**, 1823 (1995).
[14] M. P. Shaw, V. V. Mitin, E. Schöll, and H. L. Grubin, *The Physics of Instabilities in Solid State Electron Devices* (Plenum, New York, 1992).
[15] Y.-H. Shiau and Y.-F. Peng (unpublished).
[16] Recently, the group of E. Schöll also observed similar operation modes in semiconductor superlattices [see A. Amann *et al.*, Phys. Rev. B **65**, 193313 (2002); Phys. Rev. Lett. **91**, 066601 (2003); and J. Schlesner *et al.*, Phys. Rev. E **68**, 066208 (2003)].
[17] J. M. T. Thompson and H. B. Stewart, *Nonlinear Dynamics and Chaos* (Wiley, New York, 1993).
[18] C. Grebogi, E. Ott, F. Romeiras, and J. A. Yorke, Phys. Rev. A **36**, 5365 (1987).
[19] W. L. Ditto *et al.*, Phys. Rev. Lett. **63**, 923 (1989).
[20] J_{bifur} is detected when the associated values are smaller than 85 $\mu\mathrm{A}/\mu\mathrm{m}^2$.
[21] P. Yeh, *Introduction to Photorefractive Nonlinear Optics* (John Wiley & Sons, New York, 1993).
[22] R. Hall and J. H. Leck, Int. J. Electron. **25**, 529 (1968).
[23] J. Dubard, A. L. Smirl, A. G. Cui, G. C. Valley, and T. F. Boggess, Phys. Status Solidi B **150**, 913 (1989).
[24] L. Disdier and G. Roosen, Opt. Commun. **88**, 559 (1992).
[25] C.-L. Chen, *Elements of Optoelectronics & Fiber Optics* (Irwin, Chicago, 1996).
[26] In the present manuscript, the effect of the noise is to make the switching slower. Therefore, it is an undesirable effect in practice.